Involvement of Classical Bipartite/Karyopherin Nuclear Import Pathway Components in Acrosomal Trafficking and Assembly During Bovine and Murid Spermiogenesis 1

Authors: Tran, Mong Hoa, Aul, Ritu B., Xu, Wei, van der Hoorn, Frans A., and Oko, Richard

Source: Biology of Reproduction, 86(3) : 84

Published By: Society for the Study of Reproduction

URL: https://doi.org/10.1095/biolreprod.111.096842

BIOLOGY OF REPRODUCTION (2012) **86**(3):84, 1–11
Published online before print 7 December 2011.
DOI 10.1095/biolreprod.111.096842

Involvement of Classical Bipartite/Karyopherin Nuclear Import Pathway Components in Acrosomal Trafficking and Assembly During Bovine and Murid Spermiogenesis[1]

Mong Hoa Tran,[3,4] Ritu B. Aul,[3,4] Wei Xu,[4] Frans A. van der Hoorn,[5] and Richard Oko[2,4]

[4]*Department of Biomedical and Molecular Sciences, Queen's University, Kingston, Ontario, Canada*
[5]*Department of Biochemistry & Molecular Biology, University of Calgary, Calgary, Alberta, Canada*

ABSTRACT

This study arose from our finding that SubH2Bv, a histone H2B variant residing in the subacrosomal compartment of mammalian spermatozoa, contains a bipartite nuclear localization signal (bNLS) but in spite of this did not enter the spermatid nucleus. Instead, it associated with proacrosomic and acrosomic vesicles, which were targeted to the nuclear surface to form the acrosome. On this basis we proposed that SubH2Bv targets proacrosomic/acrosomic vesicles from the Golgi apparatus to the nuclear envelope by utilizing the classical bipartite/karyopherin alpha (KPNA) nuclear import pathway. To test the protein's nuclear targeting ability, SubH2Bv, with and without targeted mutations of the basic residues of bNLS, as well as bNLS alone, were transfected into mammalian cells as GFP-fusion proteins. Only the intact bNLS conferred nuclear entry. Subsequently, we showed that a KPNA, most likely KPNA6, occupies the same sperm head compartment and follows the same pattern of acrosomal association during spermiogenesis as SubH2Bv. Sperm head fractionation combined with Western blotting located this KPNA to the subacrosomal layer of the perinuclear theca, while immunocytochemistry of testicular sections showed that it associates with the surface of proacrosomic/acrosomic vesicles during acrosomal biogenesis. The identical sperm-localization and testicular-expression patterns between KPNA and SubH2Bv suggested a potential binding interaction between these proteins. This was supported by recombinant SubH2Bv affinity pull-down assays on germ cell extracts. The results of this study provide a compelling argument that these two nuclear homing proteins work in concert to direct the acrosomic vesicle to the nucleus. Their final residence in the subacrosomal layer of the perinuclear theca of spermatozoa indicates a role for SubH2Bv and KPNA in acrosomal-nuclear docking.

acrosome, gametogenesis, karyopherin alpha, sperm, SubH2Bv

INTRODUCTION

Acrosomal biogenesis occurs during the first half of spermiogenesis and can be divided into Golgi and cap phases, which are distinguished by two different phases of secretory activity of the Golgi apparatus (GA) [1–7]. Relevant to this study is the Golgi phase during which several small proacrosomic (PA) vesicles or granules, on the trans-face of the GA, coalesce to form a single larger, dense, cored acrosomic vesicle (AV) which then docks on the nuclear envelope (NE) of the spermatid nucleus via a proteinaceous layer referred to as the subacrosomal layer of the perinuclear theca (SAL-PT) [8–14]. During the cap phase, spreading of the AV over the nuclear surface is synchronous with the expansion of the underlying SAL-PT and nuclear lamina, the latter residing on the inner side of the NE [15]. Our immunolocalization studies have demonstrated that SAL-PT proteins end up in the subacrosomal region by piggy-backing on the surface of PA and acrosomic vesicles during the Golgi and cap phases of spermiogenesis [14]. Interestingly, two prominent but functionally unrelated SAL-PT proteins, SubH2Bv and RAB2A, follow this developmental pathway that supports their different involvement in vesicular targeting during acrosomal morphogenesis [8, 9].

The PT protein, SubH2Bv, is an alkali-extractable sperm head protein that resides throughout the SAL-PT of spermatozoa. With the exception of its amino terminal end, the major part of this protein's amino acid sequence resembles core histone H2B and bears a predicted three-dimensional core-helix-strand-helix histone-fold motif, which has similar DNA binding properties to that of H2B [8]. Its unique N-terminus, on the other hand, contains a predicted bipartite nuclear localization signal (bNLS), which is the subject of the present study. The bNLS is normally found on nuclear proteins of which nucleoplasmin and N1, responsible for nucleosomal assembly, are classical examples [16–18]. Therefore, the fact that SubH2Bv, both developmentally and in spermatozoa, resides in the cytoplasm makes it a surprising protein to have this motif. The classical nuclear import pathway dictates that bNLS-bearing cargoes associate with the nuclear import receptor, karyopherin α (KPNA), alternatively known as importin α [19–23]. There are six known KPNA family members in the mouse and seven in the human, and each of five members found in spermatogenesis shows a distinct mRNA expression pattern indicative of specific roles and distinct cargoes [24, 25]. These superhelical proteins have a central NLS binding domain made of 10–12 armadillo structural subunits that form a hydrophobic binding groove for monopartite and bipartite NLS [26, 27]. KPNA also contains a C-terminal CAS (cellular apoptosis susceptibility protein)-binding domain for export out of the nucleus [28] and an autoinhibitory N-terminal, karyopherin/importin β (KPNB)-binding domain [29–32]. In binding with KPNB, the two karyophilic proteins form a functional heterodimeric nuclear import complex, where KPNA works as the cargo receptor and adaptor molecule and KPNB facilitates transport to the nuclear envelope.

SubH2Bv's intimate association with the developing acrosome combined with nuclear-related motifs suggest its involvement in acrosomal-nuclear association during spermio-

[1]Supported by grants to R.O. from National Science and Engineering Research Council (RGPIN/192093) and to R.O. (MOP-84440) and F.V.H. from Canadian Institute of Health Research.
[2]Correspondence: E-mail: ro3@queensu.ca
[3]These authors contributed equally to this work.

Received: 7 October 2011.
First decision: 8 November 2011.
Accepted: 23 November 2011.

eISSN: 1529-7268 http://www.biolreprod.org
ISSN: 0006-3363

genesis. Our aim is to show that SubH2Bv, through its bNLS, targets PA and acrosomic vesicles to the nuclear envelope by binding to the nucleocytoplasmic import receptor KPNA. In support of this aim we determined the functionality of SubH2Bv's bNLS and showed SubH2B and KPNA association during acrosomal development.

MATERIALS AND METHODS

Animals

The use of animals for the studies reported herein was approved by the Queen's University Institutional Animal Care and Use Committee.

Plasmid Constructions for Testing the Functionality of SubH2bv's bNLS

Full-length coding sequence of bovine SubH2Bv cDNA was subcloned from pBK-CMV vector (Stratagene, La Jolla, CA) into the EcoRI-KpnI sites of the vector pEGFP-C (Clontech, Palo Alto, CA) to generate an in-frame fusion gene of SubH2Bv-EGFP. Primers were designed to generate the artificial EcoRI and KpnI sites at the 5′ and 3′ ends, respectively, and were 5′-GGA ATT CAT GGC CAG AAA CGT CAC CAA GAG GA-3′ and 5′-GGG GTA CCT GGA GTT TAG GAG CGG ACA TAT CG-3.′

To create mutants of the fusion gene, primer-directed mutagenesis of the SubH2Bv-GFP construct was performed using long-distance inverse PCR [33–35]. Primers were designed with artificial Sal1 sites on the 5′ ends. The sequences of the primers used were as follows: mut 1A 5′-AGA GTC GAC AAC AAGCGC TGC AGA GGA C-3′, mut1B 5′-CGA GTC GAC GGT GAC GTT TCT GCC AT-3′, mut2A 5′-AGA GTC GAC TCA CAT TCC AGC TCT GAA TC-3′, mut2B 5′-CGA GTC GAC TTT GTA GAT TGC TTT TTG GTG-3.′ The PCRs were performed using an Expand Long Template PCR Systems (Roche Biomolecular, Germany), and the single-band PCR products were band prepped using a QIA prep Gel Extraction Kit (Qiagen, Mississauga, ON), digested with Sal1, and blunt-end ligated overnight at room temperature. The resulting construct was transformed and mini-prepped for analysis.

To obtain a construct with only the NLS portion of the SubH2Bv gene fused to EGFP, a C-terminus deletion mutant of SubH2Bv-GFP fusion gene was also created by PCR. The primers were designed to exclude the C-terminus of SubH2Bv and included a restriction site for ApaI at the 5′ ends. The sequences of the primers were 5′ATA GGG CCC TGA TTT CTT TTT GTA GAT TGC-3′ and 5′GAT ATG TCC GACT CCT AAA CT-3.′ The single-band PCR product was purified, digested with ApaI, ligated overnight at room temperature, and transformed.

The sequences of all constructs created were verified by sequencing with ABI PRISM Dye Terminator Cycle Sequencing Kit with AmpliTaq DNA Polymerase (Cortec, Kingston, ON).

Cell Cultures

The established cell lines of NIH 3T3 mouse fibroblast and HEK 293 human embryonic kidney cells were cultured in Dulbecco modified Eagle medium (DMEM) supplemented with 10% fetal bovine serum at 37°C. Cells were maintained in a water-saturated incubator with 5% CO_2.

Transfections of DNA Construct in 3T3 Cells

Cells were grown on cover slips placed on the bottom of a six-well dish (9.4 cm^2 per well) to a density of 3×10^5 cells per well the night before transfection. When the cells were 60%–80% confluent, transfection was performed as follows. The plasmid DNA (2.0 ug) was diluted in 100 ul serum-free growth medium and incubated with 10 ul SuperFect Transfection Reagent (Qiagen) to allow transfection complexes to form. The transfection complexes were then incubated with the cultured cells for 2–3 h, the excess was washed off with PBS, and the cells were allowed to grow in fresh growth medium for 24–48 h. After transfection, cells were either observed directly in the culture dish (phase contrast) or fixed, and cover slips were prestained with 4, 6-diamino-2-pheylindole (DAPI) fluorescent dye and viewed with a fluorescent microscope (Axiovert 200; Zeiss, Toronto, ON).

Isolation of Pachytene Spermatocyte and Round and Elongated Spermatids

Cells were prepared according to Romrell et al. [36] and separated using a counterflow centrifugation method based on the cell's sedimentation velocity and flow rates against a vertically directed stream of liquid. DMEM was prepared with the addition of Na Lactate and Na Pyruvate and added to rat testes that had been cut and prepared on ice to expose the seminiferous tubules. Collagenase (0.5 mg/ml) was added to the sample for 15 min at 32°C, and the sample was allowed to settle afterwards. The tubules were washed three times with Krebs media, and the wash supernatant was also spun to maximize yield and retrieve any lost sample. Resuspending the sample pellet in Krebs media with trypsin (0.125 mg/ml) and DNase I (40 μg in 40 ml), the mixture was allowed to stand for 15 min at 32°C, but no longer to avoid cellular degradation. The resulting cell suspension was mixed well and checked to ensure the sample was well homogenized with no cell clusters. Trypsin inhibitor was added and the sample was filtered into a centrifuge tube, spun at room temperature for 10 min at 400 × *g*, rinsed with Krebs media, and spun again. Krebs media and DNase were added to the pelleted sample, which was loaded into a syringe for elutriation. Pachytene cells (220 fraction), round spermatids (90 fraction), and elongated spermatids (50 fraction) were separated in the elutriator, which was set at 18°C for 100 min at 475 × *g* using a Beckman J-6B centrifuge (elutriation rotor 5.2; Mississauga, ON). The rotor speed was not changed; only the buffer flow rate was adjusted (between 40 and 200 ml/min).

Isolation of Bovine Sperm Heads

As outlined in Oko and Maravei [10], bull epididymes were collected and separated into cauda and caput sections. A Tris-buffered saline (TBS) stock solution (25 mM Tris-HCl [pH 7.5], 0.9% NaCl) was prepared with 0.2 mM phenylmethylsulfonylfluoride (PMSF). The tissue was minced and filtered on ice with TBS-PMSF, and the filtrate was spun for 10 min using an angle rotor at 2500 × *g* at 4°C. The sperm pellet was washed three times in TBS-PMSF (under the same conditions), resuspended in the stock solution, and sonicated (Vibrocell Sonicator, 50W model; Sonics and Materials Inc., Danbury, CT). Three rounds of sonication were carried out in 15-sec intervals at 50 W on ice to avoid protein degradation. Phase contrast microscopy was used to verify that greater than 99% cleavage at the sperm head-tail junction had been attained. The sperm pellet was suspended and thoroughly mixed in 80% sucrose gradient and ultracentrifuged at 200 000 × *g* for 90 min in a Ti55 angle rotor (Beckman) to separate the head and tail components. The pellet on the centrifugal side of the tube was collected with TBS-PMSF and checked using phase contrast microscopy to ensure that the sample contained more than 99% sperm heads. Additional sonication and ultracentrifugation was performed as required. The isolated and sonicated sperm heads (SSpH) were again washed three times with TBS-PMSF at 2500 × *g* at 4°C and prepared for extraction.

Protein Extraction

The sonicated sperm heads were incubated with 0.2% Triton-X-100 for 1 h at room temperature with agitation, or overnight in the cold room at 4°C, to extract membrane-associated proteins. The Triton-extracted suspension was centrifuged at 2500 × *g* at 4°C to separate the extracted proteins from the remaining sperm head pellet. The isolated Triton extract was dialyzed with MWCO 6–8 kDa Spectra/Por membrane dialysis tubing (Spectrum Laboratories, Rancho Dominguez, CA) against four changes of distilled water. Alternatively, the samples were concentrated with MWCO 10 kDa ultrafiltration Centriprep tubes (Amicon, Beverly, MA) and spun at 3000 × *g* at 4°C for 30-min intervals using a fixed angle rotor. The extracts were aliquoted into 1-ml eppendorfs and lyophilized for SDS-PAGE analysis. The Triton-extracted sperm head pellet was then successively extracted with 1 M KCl to extract ionic-bound PT polypeptides [37] and 0.1 M NaOH to extract the alkali-soluble PT proteins [10].

SDS-PAGE and Western Blotting

Lyophilized extracts and isolated cells were solubilized in reducing sample buffer (2% SDS: 5% β-mercaptoethanol) and boiled for 5 min. The samples were run on 4.5% stacking and 10%–12% polyacrylamide separating mini-gels, as described by Laemmli [38], for 90 min at 120 V and compared against molecular weight standards. Low-molecular-weight markers (LMW-SDS; Amersham Biosciences, Piscataway, NJ) were used for KPNA and SubH2Bv immunoblots, while a high molecular weight marker (HMW-SDS; Amersham Biotechnology) was better suited for KPNB. The gel extract profiles were electrophoretically transferred to nitrocellulose membranes (0.45-μm pore size; Schleider and Schell, Keene, NH) or polyvinylidene difluoride microporous membranes (0.45-μm pore size; Millipore, Mississauga, ON) at 250 mA for 120 min using a Hoefer Transphor apparatus (Hoefer Scientific Instruments, San Francisco, CA) as prescribed by Towbin et al. [39]. The markers were identified with 0.1% ponceau rouge, and the membranes were washed with 25 mM PBS (pH 7.4) with 0.1% Tween-20 and blocked with 10% nonfat dry milk.

The primary antibody, prepared in 2% nonfat dry milk, was incubated for 1 h at room temperature with agitation, or overnight in the cold room at 4°C, and detected with a conjugated secondary antibody in 2% nonfat dry milk. After a 2-h incubation period at room temperature with the secondary antibody, the immunoreaction was visualized with enhanced chemiluminescent substrate (Pierce, Rockford, IL).

Antibodies

KPNA1/6 (C-20) was a commercially purchased polyclonal anti-karyopherin α antibody against the C-terminal domain of KPNA1 and A6 of human origin raised in goat (Santa Cruz Biotechnology Inc., Santa Cruz, CA). The detection by KPNA1/6 was compatible with mouse, rat, bovine and humans and used at a dilution of 1:500 for immunoblotting and 1:30 for immunoperoxidase labeling. The secondary antibody for this peptide was horseradish peroxidase conjugated rabbit anti-goat IgG (H+L) (Bio-Rad Laboratories, Mississauga, ON) used at a dilution factor of 1:10 000.

KPNB1 (H-300) was a polyclonal anti-karyopherin β1 antibody purchased from Santa Cruz Biotechnology Inc., used at 1:500 for immunoblotting and 1:30 for immunohistochemistry. KPNB1 reacts to residue 1–300 of human KPNB's N-terminal and was raised in rabbit. The secondary antibody for this protein was goat anti-rabbit IgG (H + L) (Vector Laboratories Inc., Burlingame, CA) diluted at 1:10 000. Karyopherin β1 monoclonal antibody was raised in mouse (BD Biosciences, Franklin Lakes, NJ). The monoclonal was used at 1:500 and is reactive in dog, humans, mouse, and rat and detected using conjugated goat anti-mouse IgG (H+L) horseradish peroxidase (Bio-Rad Laboratories, Mississauga, ON) at a dilution factor of 1:10 000.

Anti-SubH2Bv antibodies were affinity purified in our lab according to a protocol adapted from Oko and Maravei [10]. Rabbit antiserum raised against sperm PT extracts was used to affinity purify antibodies from Western blot-immobilized SubH2Bv. The affinity-purified SubH2Bv antibodies were concentrated two times for Western blot analysis and another 10 times for immunoperoxidase labeling of paraffin-embedded tissue. Goat anti-rabbit IgG (H + L) was used as the secondary antibody (Vector Laboratories, Inc.) to detect the protein.

Immunohistochemistry

Testis from bull, mouse, and rat were perfused in Bouin fixative, embedded in paraffin, and prepared for immunolabeling according to the protocol published by Oko [13]. Each 5-μm-thick section on a glass slide was deparaffinized with xylene and then hydrated through a graded series of ethanols. Once hydrated, the sections were subjected to antigen retrieval if needed by microwaving in a 0.01 M sodium citrate solution, pH 6 (for details, see [40]). To minimize nonspecific binding, the sections were blocked with 10% normal goat serum (NGS) for 15 min. The primary antibody was then added, and the tissue samples were incubated for 1.5 h at room temperature or overnight at 4°C. Subsequently, the sections were washed with TBS containing 0.1% Tween-20, blocked with 10% NGS, and incubated with biotinylated secondary antibody for 30 min prior to incubation with Immunoperoxidase avidin-biotin reagent (ABC; Vectastain Elite ABC Kit; Vector Laboratories). To elicit the immunoperoxidase reaction, 0.5% diaminobenzidene tetrahydrochloride in TBS containing 0.1 M imidazole and 0.03% H_2O_2 was used. The tissue was then counterstained, dehydrated into xylene, and mounted with permount (Fischer Chemicals, Fairlawn, NJ).

Construction and Expression of Recombinant SubH2Bv

Bull recombinant SubH2Bv and primers were prepared from SubH2Bv's cDNA (GenBank Accession No. bankit36366 AF315690) and amplified using Qiagen Taq PCR kit (Qiagen). Two primers were designed by Cortec Technologies—a 24-bp primer with a nucleotide sequence of 5′-GAGCT′ CAATGGCCAGAAACGTCAC-3′, which included a 5′-GAGCT′C-3′ SAC 1 site, and a 23-bp primer sequence 5′-GC′GGCCGCGGAGCGGA CATATCG-3′, with an incorporated 5′-GC′ GGCCGC 3′ NOT 1 site. The ′ indicates the cut site for the restriction enzymes.

A mastermix containing 5 μl of 10× PCR buffer, 1 μl dNTP, 10 μl of 25 mM $MgCl_2$, 5 μl of each primer, and 0.4 μl of Taq DNA polymerase was prepared and added to 23.1 μl of ddH_2O and dispensed into PCR tubes. The SubH2Bv cDNA was added and placed in the thermal cycler that alternated between 94°, 52°, and 72°C. In this instance, annealing was optimized at 52°C. A DNA band of approximately 381 bp was visualized in a 2% agarose gel stained with ethidium bromide. The PCR products were cloned with the Qiagen Cloning Kit (Qiagen) into pDrive Cloning Vectors. A ligation-reaction mixture was added, and the suspension was incubated for 2 h at 16°C.

Transformation was carried out with Qiagen EZ competent host cells (Qiagen), and ampicillin LB agar plates were prepared (1 μl/ml LB). Ligation reaction mixture was added to each tube of competent cells, incubated on ice for 5 min, then heat-shocked with a hot water bath for 30 sec at 42°C. SOC medium (Sigma-Aldrich, Oakville, ON) was added to each tube, and the transformation mixture was plated and incubated. Colonies were selected and tested on 2% agarose for the insert.

The inserts and expression vectors were linearized for subcloning with SAC 1 and NOT 1 restriction enzymes, incubated for 2 h at 37°C. The inserts were subcloned and expressed in pet21b (+) expression vectors from Novagen (Madison, WI) for 30 min and transformed in *E. Coli* BL21 DE3 [PlyS] cells (Novagen) using the above protocol.

Protein Purification and Affinity Pull-Down

His-tagged recombinant SubH2Bv (recSubH2Bv) was immobilized on Ni-NTA-charged beaded agarose (Qiagen) to bait KPNA obtained from 0.1% Triton-extracts of isolated sperm heads. Two ml of *E. coli* cell culture was collected, sonicated, and spun down to produce the pellet containing the insoluble recombinant peptide and denatured with 8 M urea (100 mM NaH_2PO_4, 10 mM Tris, pH 8) overnight in the cold room (4°C). The suspension was spun and cleared, and the supernatant with the solubilized recSubH2Bv was incubated with 10 μl of Ni-NTA agarose for 4 h at 4°C. The Ni-slurry was washed five times with TBS containing 10 mM Imidazole (pH 8) and spun. The immobilized SubH2Bv on Ni beads was then incubated with 500 μl of Triton extract, obtained from isolated sonicated sperm heads for 4 h in the cold room, spun, and washed five times with TBS with 10 mM Imidazole. The proteins were eluted twice with 2× reducing sample buffer and detected on Westerrn blots for SubH2Bv and KPNA.

RESULTS

SubH2Bv Directs Nuclear Entry of EGFP into Somatic Cells

To determine the subcellular localization of SubH2Bv in somatic cells, a fusion gene of EGFP and SubH2Bv was constructed under the control of the immediate early promoter of CMV. The expression vector, pEGFP-SubH2Bv, was transfected into 3T3 mouse fibroblasts and visualized by confocal microscopy. The enhanced green fluorescent signal was detected mainly within the cell nuclei, as visualized by DAPI staining (Fig. 1A). Results obtained in the human embryonic kidney cells were identical (not shown).

SubH2Bv's bNLS Confers Nuclear Specificity

Amino acid sequence analysis revealed that SubH2Bv coded a series of amino acids in its N-terminus typical of the classical bNLS sequence, made up of two basic clusters tethered by a string of 10–12 amino acids [8].

To test the function of this predicted bNLS (a.a., 7–23), a fusion gene of the N-terminus (a.a., 1–24) of SubH2Bv and EGFP was constructed and transfected into 3T3 cells. Transfection of this C-terminal deletion construct enhanced nuclear localization of EGFP (Fig. 1B), indicating that SubH2Bv's bNLS was the predicted motif, conferring nuclear localization of SubH2Bv into somatic cells. This contrasted with EGFP control results, where the green fluorescence was visualized throughout the entire cell (Fig. 1C).

Mutation of the bNLS Obliterates SubH2Bv's Nuclear Entry

To confirm the functionality of the bNLS in SubH2Bv, fusion proteins containing selectively mutated basic residues of the bNLS within SubH2Bv were created and transiently transfected in the cell lines. The first mutated construct (mutant #1) contained two amino acid substitutions, resulting in the replacement of the upstream basic cluster of KR (a.a., 7, 8) with VD. The second mutant (mutant #2) also contained two amino acid substitutions, resulting in altering the downstream cluster of KKK (a.a., 22, 23) with KVD. Both mutated fusion proteins failed to efficiently enter the nucleus of the cultured cells and instead congregated as cytoplasmic clumps (Fig. 1, D

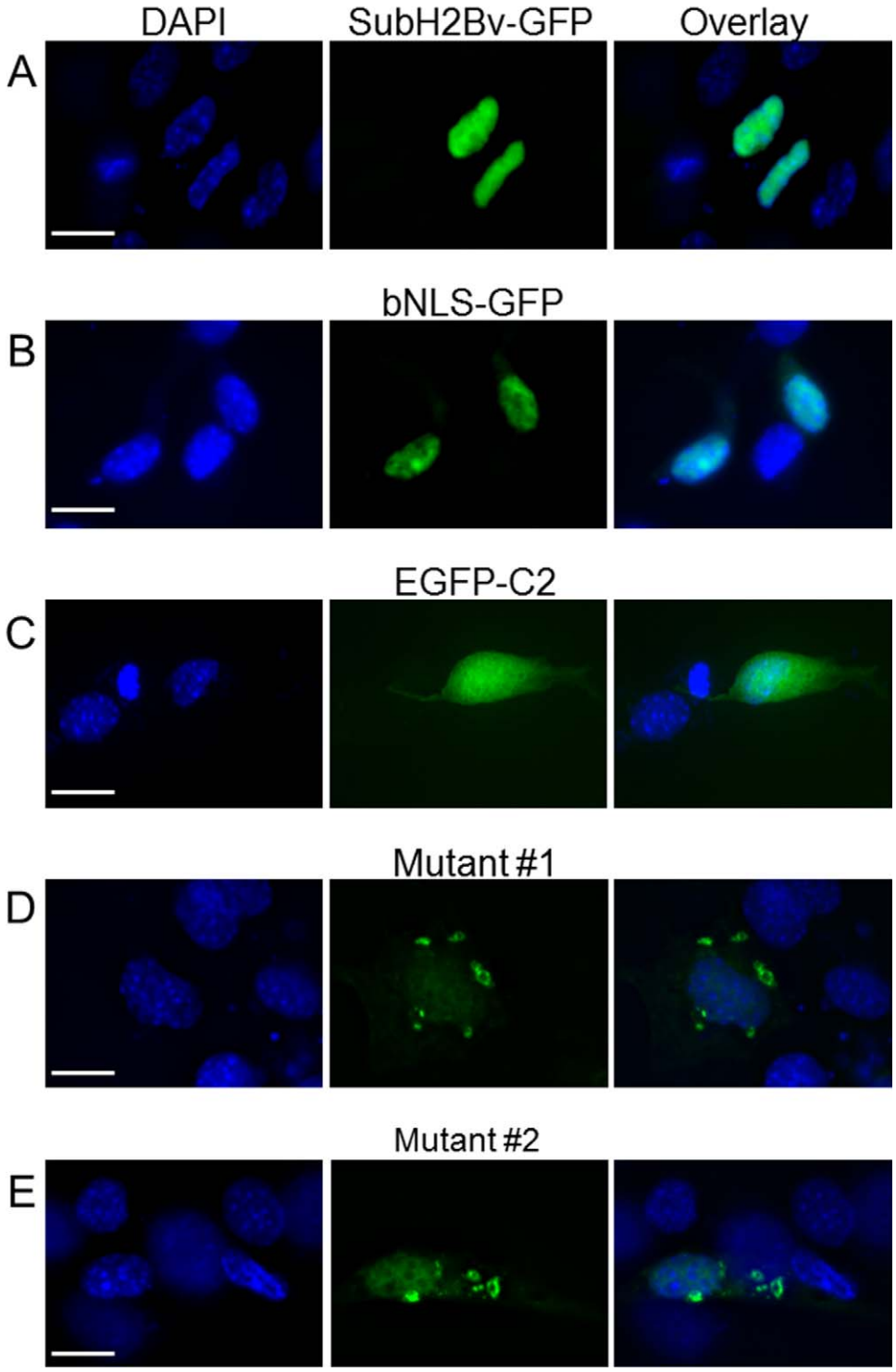

FIG. 1. Subcellular localization of GFP fused with either whole SubH2Bv (**A**) or the N-terminus of SubH2Bv (1MARNVTKRKNRCRGHQKAIYKKKS24), containing the intact bNLS (**B**). Subcellular localization of GFP alone (**C**). Subcellular localization of GFP fused with SubH2Bv containing mutants (#1 and #2) of the bNLS motif (**D**, **E**). In mutant #1 (1MARNVTVDKNRCRGHQKAIYKKKS . . . 122) the upstream basic cluster KR was substituted with VD (**D**). In mutant #2 (1MARNVTKRKNRCRGHQKAIYKVDS . . . 122) the downstream basic cluster KK was substituted with VD (**E**). Expression vectors of the fusion genes were transfected into 3T3 mouse fibroblast cells, and then the cells were cultured for 24–48 h before being stained with DAPI and examined by confocal fluorescent microsocopy. Bars = 10 μm.

and E). Altering either of the basic clusters in the bNLS obliterated nuclear entry in an identical manner, providing evidence that SubH2Bv, through its bNLS, can bind to the nucleocytoplasmic import receptor KPNA and acts as a karyophilic cargo molecule.

Karyopherin α Is a Constituent of the Sonication-Resistant, Isolated Sperm Head Fraction

Because the SSpH fraction is enriched in the PT proteins SubH2Bv, RAB2A, Calicin and the four somatic histones, it

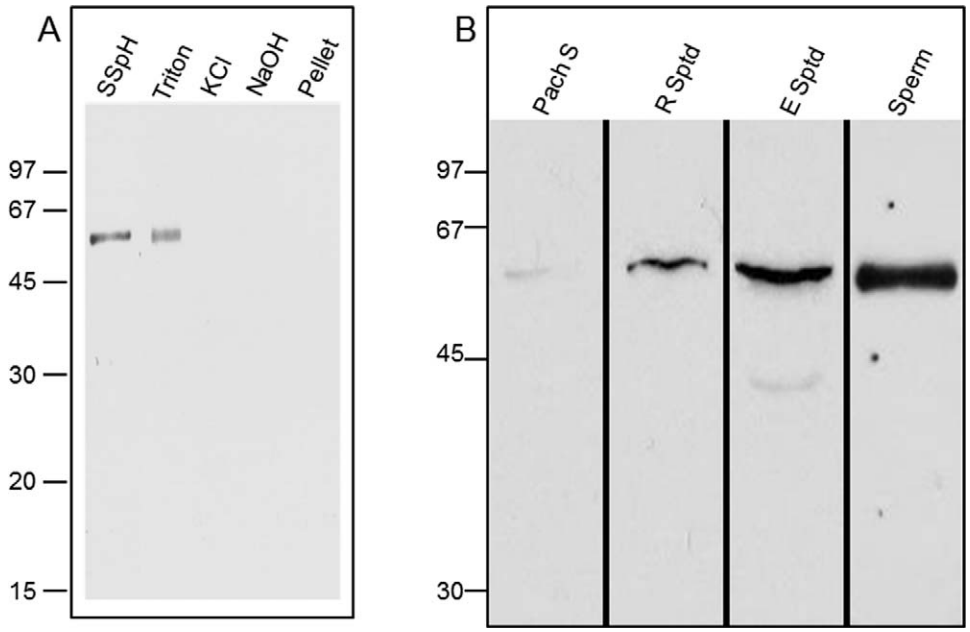

FIG. 2. **A**) Western blot of SSpH and sequential extractions of SSpH (i.e., 2% Triton X-100, 1 M KCL, and 0.1 M NaOH) immunolabeled with anti-KPNA1/6 antibody. **B**) Western blot of elutriated rat testicular germ cells immunolabelled with anti-KPNA1/6 antibody. The cells including mature spermatozoa (sperm) were loaded at approximately equal numbers per cell lane. Values are kDa. Pach S, pachytene spermatocytes; R Sptd, round spermatids; E Sptd, elongated spermatids.

was used to determine if a KPNA was also confined to this SSpH fraction by Western-/immunoblotting. Indeed, an anti-KPNA antibody (anti-KPNA 1/6) recognized a single 60-kDa band, consistent with the reported molecular mass of KPNA1 or A6 (KPNA1/6), in bovine (Fig. 2A) and rat (not shown). To determine its binding characteristics, sequential extracts of 2% Triton-X100, 1 M KCL, and 0.1 M NaOH were performed on the SSpH fraction. KPNA1/6 was extractable from SSpH with Triton X-100 and not present in subsequent KCL and NaOH extracts or in the final pellet (Fig. 2A). This suggests a hydrophobic association with either IAM and NE and/or proteins associated with the SAL-PT.

Karyopherin α Is Enriched in Isolated Spermatids

To demonstrate that a KPNA was present in spermatids during acrosomal biogenesis, germ cell fractions, consisting of pachytene spermatocytes, round spermatids, and elongated rat spermatids (estimated 85%, 85%, and 60% purity for each fraction, respectively), were purified by centrifugal elutriation. Immunoblots of these three germ cell fractions showed that KPNA1/6 was more abundant in round spermatids at the time of acrosomal morphogenesis and in elongated spermatids than in pachytene spermatocytes (Fig. 2B), confirming our suspicion of developmental immunohistochemical localization during spermatogenesis.

Karyopherin α Is Associated with Acrosome Formation During Spermiogenesis

In order to determine the localization of KPNA in round spermatids and obtain a chronology of this protein's predicted association with acrosomal morphogenesis, immunoperoxidase immunocytochemistry was performed on deparaffinized testicular sections using anti-KPNA1/6 antibody. KPNA, like SubH2Bv [8], was mainly localized to the spermatid cytoplasm, where it associated with the secretory vesicles forming the acrosome in all three species investigated (i.e., mouse, rat, and bull; Figs. 3 and 4 and Supplemental Fig. S1, available online at www.biolreprod.org). In these testicular sections, immunoperoxidase staining clearly demarcated the surface of PA vesicles in step 2 of spermiogenesis as they began to fuse to form the AV and migrate to the nuclear envelope (Fig. 3, A and B). In step 3 spermatids, the fusion of the PA vesicles was complete, and the immunoperoxidase-reaction product now covered the surface of the AV as it attached to the NE of the spermatid (Fig. 4A). At the beginning of the cap phase of spermiogenesis (step 4), KPNA-immunoperoxidase staining initially expanded around the surface of the growing AV (Fig. 3C) but by step 5 had become diminished from the outer acrosomal membrane surface and concentrated between the inner acrosomal membrane and NE in the subacrosomal margin (Figs. 3D and 4B). From steps 6 to 8, KPNA antigenicity expanded with the increase in size of the subacrosomal margin as the acrosome capped the nucleus (Fig. 4C). During spermatid elongation, KPNA-immunoperoxidase staining was present over the sperm nucleus in the region covered by the acrosome (Fig. 4D). Normal rabbit serum was used as a control and showed either little or no immunoperoxidase immunoreactivity (see Supplemental Fig. S1).

Sperm Karyopherin α and SubH2Bv Have a Binding Affinity

SubH2Bv's functionally active bNLS, coupled with near-identical sperm-localization and testicular-expression patterns of SubH2Bv [8] and KPNA1/6 (this study), suggested that a binding interaction exists between these proteins. To establish a protein-protein interaction between these proteins, recombinant His-tagged SubH2Bv was stabilized on Ni-agarose beads and used in an affinity pull-down assay to bait KPNA in germ cell extracts. Traditional immunoprecipitation could not be used because of the insoluble nature of SubH2Bv within the germ cell. Immunoblots of Triton X-100-extracts of SSpH (Tx, Fig. 5, lane 1) and Ni-conjugated, affinity-purified recombinant

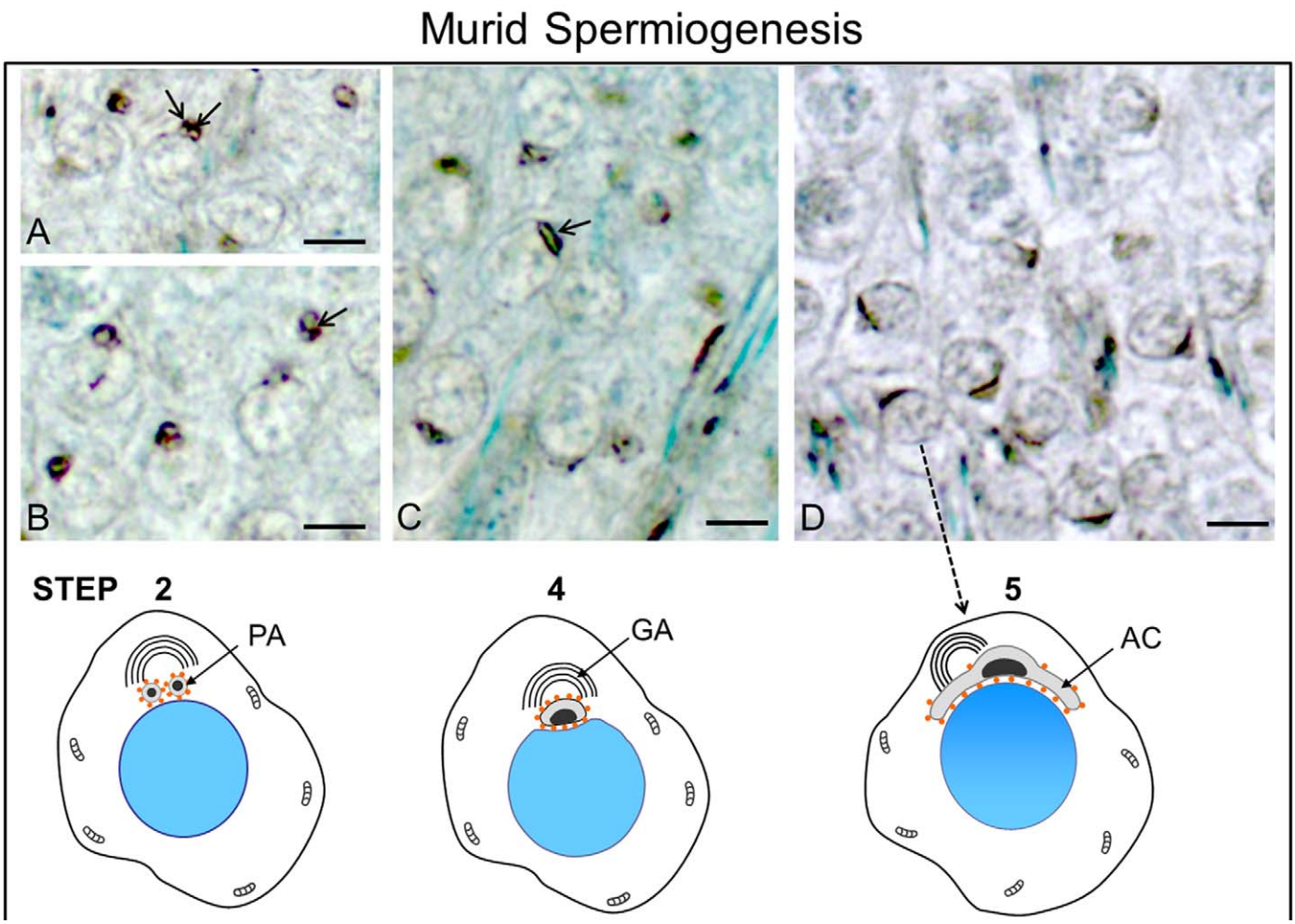

FIG. 3. Murid (rat and mouse) testicular sections immunoperoxidase stained with anti-KPNA1/6 antibody counterstained with methylene blue. KPNA-immunoreactive PA vesicles fuse with each other (arrows) in step 2 of spermiogenesis (**A**, **B**). The fusion of these vesicles results in a larger acrosomic vesicle (arrow), which by step 4 has firmly attached to the spermatid nucleus and is beginning to expand over it (**C**). KPNA immunoreactivity is clearly seen associated with the periphery of these vesicles. By step 5 in spermatids, the immunoperoxidase staining predominates in the subacrosomal margin (between the inner acrosomal membrane and NE) or the PT (**D**). A diagrammatic interpretation of KPNA's association (orange dots) with the developing acrosome in respective spermatids is displayed below in this and the subsequent figure. GA, Golgi apparatus; AC, acrosomal cap. Bars = 5 μm.

SubH2Bv (SubH2Bv-Ni, Fig. 5, lane 3) served as positive controls for KPNA and SubH2Bv, respectively, while immunoblots of Tx incubated with the Ni-beads (Tx-Ni, Fig. 5, lane 2) demonstrated that nonspecific binding of KPNA to the Ni-beads did not occur (Fig. 5). Furthermore, immunoblots of Tx incubated with the Ni-conjugated recombinant SubH2Bv (Tx-SubH2Bv-Ni;, Fig. 5, lane 4) showed a binding affinity between KPNA1/6 and SubH2Bv.

Karyopherin β Is a Constituent of the SSpH and Present in Round Spermatids

Since the relationship between KPNA and Karyopherin β (KPNB) as transport heterodimers for bNLS-cargo was demonstrated, we further determined whether KPNB1 was present in the same sperm and testis locations as KPNA1/6. Immunoblots using a monoclonal antibody against KPNB1 identified KPNB1 as a detergent-extractable protein of SSpH and a constituent of isolated round spermatids (Fig. 6). This supported KPNB1's association with acrosomal morphogenesis, previously shown by Yang and Sperry [41].

DISCUSSION

Spermiogenesis is a cytomorphogenic event that takes place toward the end of spermatogenesis [2, 3]. During this time, the sperm cell's unique shape and structural features, comprising the acrosome, an enzymatic secretory vesicle capping the highly condensed nucleus, the PT, a proteinaceous layer of scaffolding for the overlying acrosome, and the sperm tail, a contractile axoneme surrounded by accessory fibres, develop. The acrosome has a unique distinction in that it houses the components needed for binding to and penetrating the oocyte coat, providing the leading edge for this process [42]. Though much is known of the morphology and development of the acrosome, the mechanisms that deliver the secretory vesicles from the Golgi apparatus to the nuclear envelope and attach it to this membrane are unexplored. Past studies have identified V-snare VAMPS, t-snare syntaxins, RABs, clathrin, and β-COP as acrosomal-associated surface proteins [43, 44], and even though these proteins most likely play an important role in vesicular trafficking, fusion, and sorting, none to our knowledge have been implicated in targeting the PA and acrosomic vesicles to the NE. SubH2Bv, encoded with a bNLS

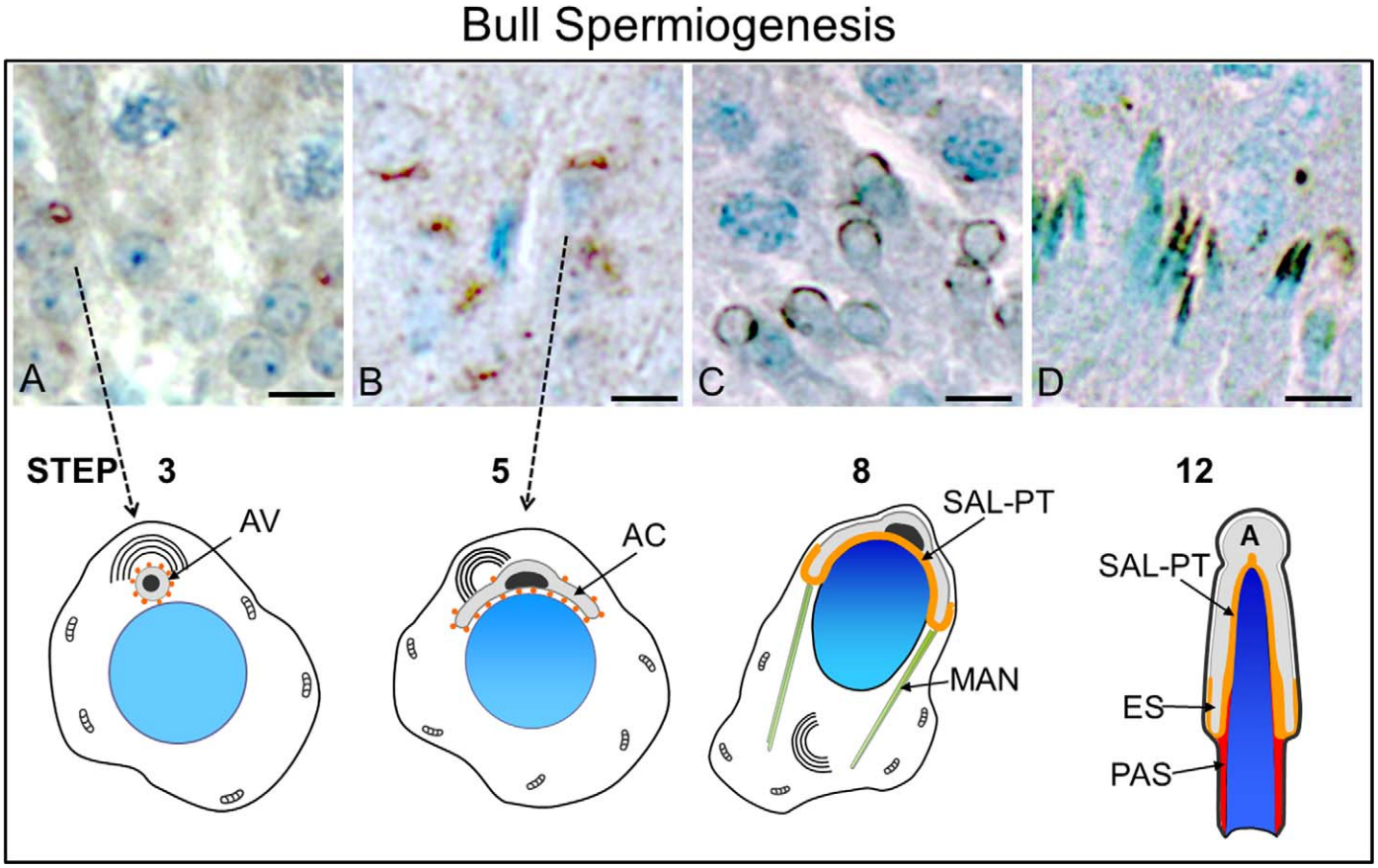

FIG. 4. Bull testicular sections immunoperoxidase stained with anti-KPNA1/6 antibody. As in the murid, KPNA immunoreactivity is associated with the surface of the AV in step 3 spermatids and concentrated in the subacrosomal margin or PT of step 5 spermatids (**A**, **B**). During spermatid elongation, KPNA reactivity is retained over the sperm nucleus (N) in the region covered by the acrosome (**C**, **D**). AV, acrosomic vesicle; AC, acrosomal cap; SAL-PT, subacrosomal layer of perinuclear theca; MAN, microtubular manchette; ES, equatorial segment; PAS, postacrosomal sheath. Bars = 5 μm.

and being a major constituent of the SAL-PT [8], appears to be a prime candidate involved in the nuclear targeting and attachment of the acrosome.

Transfection analysis with SubH2Bv-GFP fusion proteins demonstrated two interesting characteristics about SubH2Bv. First, SubH2Bv enters the nuclei of somatic cells but not, it would seem, the nucleus of the developing spermatid [8]. Second, the amino acids comprising the bNLS are responsible for conferring the nuclear specificity. The bNLS is defined by two adjacent basic amino acids and a spacer region of 10–12 residues, followed by at least three basic residues [45, 46]. We found that replacing two basic residues with two nonbasic residues in either of the basic clusters of the bNLS obliterates nuclear entry of SubH2Bv. In comparison to the control, the bNLS of SubH2Bv was able to redirect EGFP, which normally, when transfected alone, is present throughout the somatic cell, almost entirely into the nucleus. Studies similar to ours on other proteins containing the bNLS showed that the two basic up- and down-stream clusters are interdependent, while the spacer region has little or no effect on nuclear localization [18, 45–47]. The C-terminal and bipartite domain mutants of SubH2bv support the view that the N-terminus encodes a functional, bipartite, nuclear targeting sequence.

The vast majority of proteins containing a functional bNLS are destined to enter the nucleus [48]. This NLS-mediated nucleocytoplasmic transport requires four discrete steps: binding of the NLS protein with importin α (KPNA), complex formation with importin β (KPNB), targeting to the nuclear pore complex (NPC), and Ran/GTP-mediated translocation through the NPC [49]. With the functionality of SubH2Bv's bNLS determined in the current study and the observation that SubH2Bv coats the PA and acrosomic vesicles during their transit to and docking of the NE [8, 15], we hypothesized that SubH2Bv uses its NLS to target these secretory vesicles toward the nuclear envelope, especially as the mechanism of secretory targeting of the nuclear envelope is germ cell-specific and unknown. We reasoned that, for this hypothesis to have merit, a conditional requirement would be to demonstrate that one of the seven KPNA family members [24] follows an identical targeting pathway to SubH2Bv during acrosomal biogenesis. KPNA members are nucleocytoplasmic transport receptors that bind to bNLS cargoes with great affinity [50]. Normally, for KPNA and its cargo to be transported towards the nucleus, it binds through its N-terminal importin β binding domain (IBB) to KPNB to form a functional ternary transport unit [19, 51], although there are a few exceptions where KPNA has been shown to transport cargo to the NE independently of KPNB [52, 53]. Though KPNB is capable of binding nonclassical NLS-bearing peptides, its main function when complexed with KPNA is to target and dock the trimeric unit to nuclear pores for subsequent nuclear import [20, 32]. KPNA's central adaptor role in forming the ternary nuclear transport unit therefore provides an underlying mechanism and explanation for SubH2Bv's presence on PA and acrosomic vesicles.

From our immunolocalization data it appears that a KPNA coats the PA and acrosomic vesicles similar to that of SubH2Bv during the round spermatid phase of spermiogenesis [8]. Since the anti-karyopherin α antibody (KPNA1/6) used for

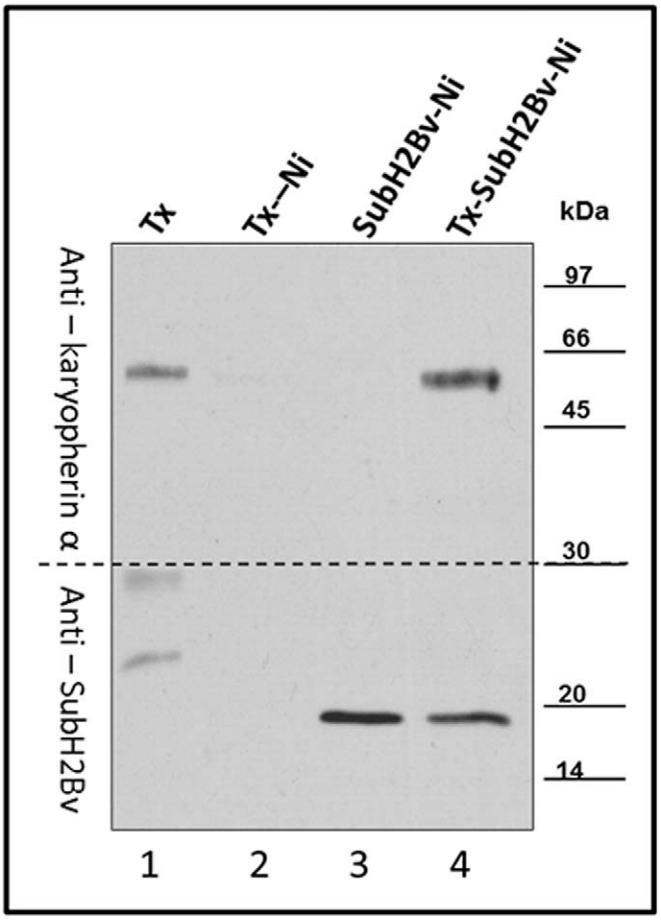

FIG. 5. Affinity pull-down of sperm-extracted KPNA with recombinant SubH2Bv detected by immunoblotting using anti-KPNA1/6 and anti-SubH2Bv antibodies. SSpH were extracted using 0.1% Triton X-100 (Tx). Lane 1: Triton extract (Tx) alone showed labeling of a 60-kDa band as expected; lane 2: Tx purified over a Ni column (Tx-Ni) showed no labeling; lane 3: His-tagged recombinant SubH2Bv purified over a Ni column (SubH2Bv-Ni) showed labeling of a 15-kDa band as expected; lane 4: Tx pre-incubated with SubH2Bv and then purified over a Ni column (Tx-SubH2Bv-Ni) showed labeling of both KPNA1/6 and SubH2Bv.

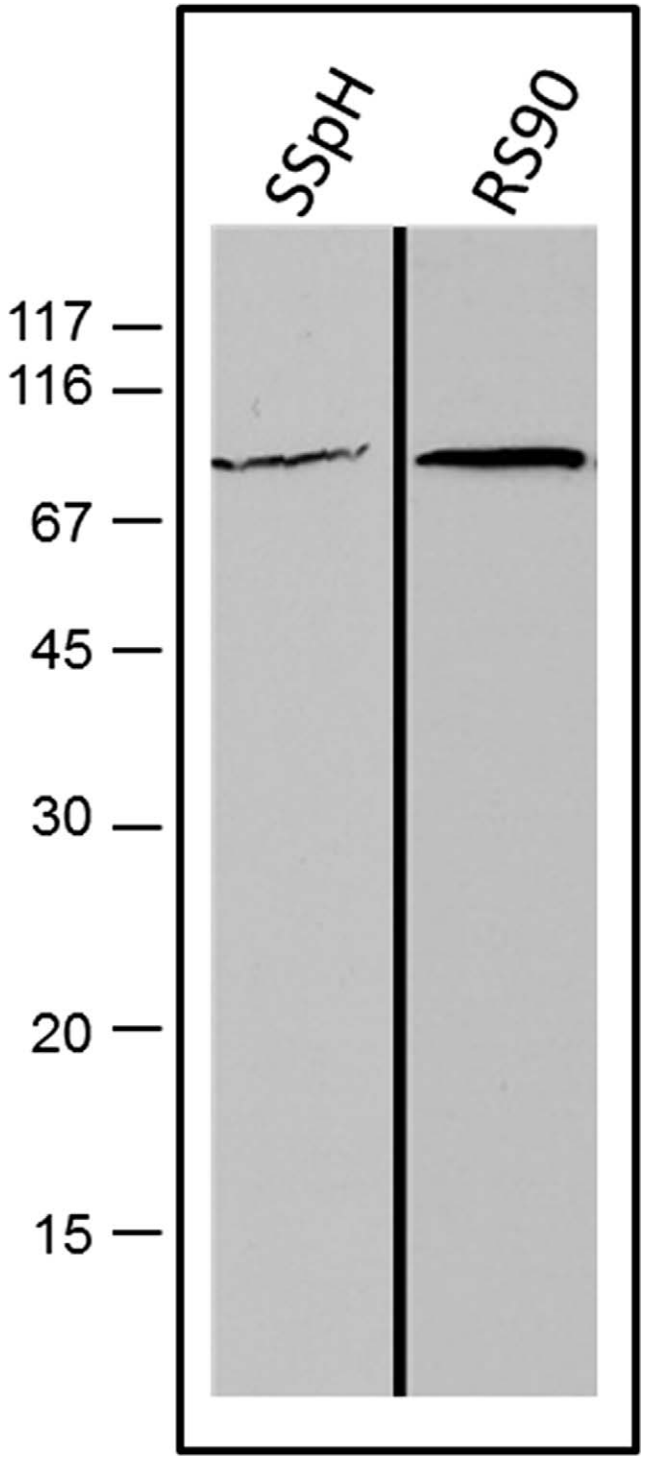

FIG. 6. Western blots of detergent extract of SSpH and elutriated round spermatid fraction (RS90) immunolabeled with anti-KPNB1 monoclonal antibody. Results were identical using KPNB1 (H-300), a polyclonal anti-KPNB1 antibody.

localization did not distinguish between KPNA family members A1 and A6, which have a similar structure and molecular mass, the possibility exists that the KPNA in question could be either A1 or A6. However, the distinct mRNA expression patterns exhibited between *a1* and *a6* during spermatogenesis suggest that *Kpna6* is the most likely candidate. Unlike *Kpna1* mRNA, *Kpna6* mRNA was detected in round spermatids from stages 1 through 8, the time period corresponding to acrosomal biogenesis [25]. Furthermore, the results from real-time PCR used to determine the levels of *Kpna1* and *Kpnaa6* mRNAs in total testis RNA indicated that the number of *a1* mRNA molecules was at least 100-fold lower than the number of *a6* molecules [25]. As was the case for SubH2Bv [8], KPNA expression originated in the Golgi phase of spermiogenesis at the time of PA vesicle formation, and the protein's intimate association with the acrosomic system was evident in both bovine and murid spermiogenesis. Even in mature spermatozoa our combined biochemical fractionation and immunoblotting analysis identified KPNA's presence in the cytosolic compartment of the sperm head where SubH2Bv resides. The sperm head fraction from which we extracted KPNA consisted solely of the sonication-resistant IAM, PT (the only cytosolic compartment remaining), NE, and nucleus. Nonionic detergent extraction of the sperm head fraction solubilized the IAM and NE and released KPNA. Most likely KPNA was released from the cytosolic compartment of the sperm head fraction, as it is a cytosolic protein and was observed coating the cytosolic side of the AV during spermiogenesis.

The similar sperm head compartmentalization and developmental pattern observed indicated that a binding interrelationship between SubH2Bv and KPNA exists within the germ cell for the purpose of nuclear targeting. We were not able to test this binding interrelationship directly by immunoprecipitating the respective proteins from germ or sperm cell extracts, as SubH2Bv proved to be insoluble in detergent extracts. However, by anchoring recombinant SubH2Bv to beads as bait we were able to effectively pull down KPNA from germ or sperm cell extracts, indicating an affinity between these proteins. The binding of these two sperm proteins led to the following hypothesis: SubH2Bv coats the PA and acrosomic vesicles and binds to KPNA (most likely A6) as its karyophilic cargo through its bNLS. The whole complex then is transported to the nuclear envelope through the KPNA/KPNB heterodimer, following the classical nuclear import pathway [51], or independently through KPNA alone [53].

We suggest that acrosomal vesicle transport favors the classical nuclear import pathway for the following reasons. First, as determined by our study, KPNB is in the same sperm compartment as both KPNA and SubH2Bv, and it is also present in round spermatids at the time of acrosome formation. Secondly, Yang and Sperry [41] carried out an immunofluorescence study with KIFC1 (a C-terminal kinesin motor protein) and KPNB1 that showed specific curvilinear colocalization of both proteins to the apical nuclear surface of round spermatids in the region of acrosome morphogenesis. They also showed by co-immunoprecipitation experiments on testicular lysates that KPNB1 and KIFC1 had a binding affinity for each other similar to KPNA and SubH2Bv in our study. The localization of KPNB1 and KIFC1 coincided with our localization of SubH2Bv and KPNA during the round spermatid phase of spermiogenesis, supporting our theory of a SubH2Bv/KPNA-mediated acrosomal transport pathway for PA vesicles. Based on the convention of bipartite/KPNA/KPNB nucleocytoplasmic transport, and backed by the findings of Yang and Sperry [41], our conceptualized model for acrosomic vesicular transport would have KPNA effectively functioning as the intermediary receptor that would recognize and bind SubH2Bv-coated acrosomic cargo and work in tandem with KPNB. Using KPNB-bound-KIFC1 as the motor for retrograde transport along the microtubules, the trimeric transport complex would then be transported to the NE for attachment. Complying with this transport route, it was shown that microtubule disruption in *azh* mice or nocodazole-treated round spermatids suppressed Golgi to acrosome trafficking [54].

Our immunolocalization results with KPNA, as similar to previous results for SubH2Bv, KPNB, and KIFC1, showed redistribution of KPNA from coating the periphery of PA and acrosomic vesicles to what appears as a linear convergence at the subacrosomal margin (between the IAM and NE), which was retained in spermatozoa. Confirmation of this developmental redistribution of KPNA awaits a higher resolution immunocytochemical study by electron microscopy. The nuclear exclusion of KPNA, SubH2Bv, and KPNB and their permanence in the subacrosomal layer of the PT suggests that they may also have a further function, in addition to their conventional signaling and transport role, in acrosomal docking and stabilization. Import-mediated nuclear localization requires docking to the NPC. However, in round spermatids NPCs disappear from the apical pole of the nucleus at the time of AV attachment to the NE [55–57]. This conclusion was based strictly on morphological observations of nuclear pore-like perforations in the NE. More recently, immunofluorescent colocalizations of specific nucleoporins and PT proteins have shown that NPCs redistribute to the caudal region of the round spermatid nucleus well before the acrosome begins to flatten over the apical pole of the nucleus [40, 58]. Conventionally, KPNB would dock the karyophilic trimeric targeting complex to nuclear pores, via nucleoporins, for subsequent nuclear import. However, since the nuclear pores that KPNB normally docks to are not present, having migrated to the caudal pole of the spermatid nucleus during the Golgi phase of spermiogenesis, another related mechanism of attachment would be expected to prevail. Molecular characterizations of the male germ cell NE provide evidence that there are testis-specific isoforms of nucleoporins and nuclear pore-associated proteins that remain associated with the NE in the absence of NPC [59–61]. One of these, NUP50 (also known as Npap 60), persisted in the apical region of the NE of round spermatids when the NPC progressed caudally [60]. A yeast two-hybrid system used to screen a mouse testis cDNA library to identify proteins capable of interacting with a testis-specific nucleoporin (BS-63) identified RAN, transportin (karyopherin β2), two proteins related to the nucleocytoplasmic transporter, and a F10 protein [59]. The gene knockout of another nucleoporin-like protein, AGFG1 (Hrb/hRip) [62], resulted in acrosome-deficient mice [61]. Therefore, it is possible that the putative trimeric complex made up of SubH2Bv, KPNA, and KPNB anchors to the NE of round spermatids via nontraditional, testicular variants of nuclear surface proteins, thereby docking the acrosome to the nucleus. Little is known about the binding interaction that happens between the nucleoporins of the NPC that helps dock and traffic KPNB and its cargo from the cytosol to the nucleus. It is generally accepted that the nucleoporin FG repeats (free from phenylalanine-guanine sequences) bind to the external, shallow hydrophobic pockets on the convex surface of KPNB to tether and subsequently import the protein and binding partners into the nucleoplasm [63]. Based on our sperm fractionation/extraction experiments in which the karyopherins are released from the sperm head under relatively mild extraction conditions compared to SubH2Bv (nonionic detergent vs. NaOH extraction), it is possible that KPNB would only serve in the initial anchoring of the AV to the NE of the spermatid until a more permanent covalent binding occurs through SubH2Bv and/or other abundant PT proteins such as RAB2A.

Though there are proponents of an acrosomal docking theory that revolves around a transient keratin-actin-based structure referred to as the acroplaxome [64, 65], we have been unable to substantiate this model [15]. The acroplaxome theory claims that there is a transient perinuclear structure, made up of actin and keratin, that appears on the NE surface prior to AV attachment and serves to dock the AV to the NE. Using a combined ultrastructural and immunocytochemical approach, we were not able to visualize the acroplaxome. Our analysis showed that the PT is seen only at the time the AV docks to the NE, as an intervening substance between these two membrane systems, and is made up of the same proteins that coat the PA and acrosomic vesicles during transport to the spermatid nucleus [8–12, 14]. Furthermore, by using an inducible mouse model of male infertility in which membrane fusion of Golgi-derived PA vesicles destined for acrosome formation was blocked (i.e., no AV formed), we observed that PA vesicles alone were still capable of docking to the NE but that there was no trace of acroplaxome or PT lining the NE between the randomly attached vesicles [66]. These observations suggest that the vesicles supply the subacrosomal material, which is retained in spermatozoa as the PT. However, a receptor on the NE would still be a requirement, which based on our study could be a nucleoporin-like protein that specifically binds with

KPNB of the trimeric karyophilic complex, whose purpose would be to target and attach the AV to the NE. Even though the acrosome did not form in our inducible mouse model of male infertility, the nuclear lamina, which directly underlies the NE, continually expanded during the Golgi and cap phases, delineating the region of the NE where docking and capping of the AV would have taken place. It is conceivable, therefore, that the nuclear lamina's presence influences or signifies a molecular change in the overlying NE that allows for acrosomal attachment.

Our data suggest that there is a direct attachment between the PT proteins that coat the PA and acrosomic vesicles (i.e., SubH2Bv, KPNA, and KPNB) and a receptor complex in, or on, the NE, which remains to be identified. In this context consideration should be given to a novel testis-specific SUN domain protein (SPAG4L-2), a transmembrane protein restricted to the apical nuclear region of round spermatids that faces the AV, as a possible component of a protein linkage complex that anchors the AV to the nuclear membrane [67]. It is well documented that SUN and KASH domain proteins, spanning the nuclear envelope, organize a diversity of nucleo-cytoplasmic connections, including tethering microtubules and centromeres to the nuclear envelope [68]. In summary, our study suggests that the traditional karyopherin/importin nuclear import pathway has been adapted in haploid spermatids to serve as an intracytoplasmic transport pathway, targeting SubH2Bv-coated secretory vesicles to the nuclear surface for acrosomal assembly. A precedent for intracytoplasmic transport and regulation of proteins by importins and RAN GTP was set by the discovery that cellular RAN GTP and importins are found in cilia and centrosomes and that they regulate the import of ciliary proteins containing NLS [69–73].

REFERENCES

1. Clermont Y, Tang XM. Glycoprotein synthesis in the Golgi apparatus of spermatids during spermiogenesis of the rat. Anat Rec 1985; 213:33–43.
2. Clermont Y, Oko R, Hermo L. Cell and molecular biology of the testis In: Desjardins C, Ewing L (eds.), Cell Biology of Mammalian Spermatogenesis. New York: Oxford University Press; 1993;332–376.
3. Oko R, Clermont Y. Spermiogenesis In: Knobil E, Neill JD (eds.), Encyclopedia of Reproduction, vol. 4. San Diego: Academic Press; 1998;602–609.
4. Smith CE, Hermo L, Fazel A, Lalli MF, Bergeron JJ. Ultrastructural distribution of NADPase within the Golgi apparatus and lysosomes of mammalian cells. Prog Histochem Cytochem 1990; 21:1–120.
5. Susi FR, Leblond CP, Clermont Y. Changes in the golgi apparatus during spermiogenesis in the rat. Am J Anat 1971; 130:251–267.
6. Tang XM, Lalli MF, Clermont Y. A cytochemical study of the Golgi apparatus of the spermatid during spermiogenesis in the rat. Am J Anat 1982; 163:283–294.
7. Thorne-Tjomsland G, Clermont Y, Hermo L. Contribution of the Golgi apparatus components to the formation of the acrosomic system and chromatoid body in rat spermatids. Anat Rec 1988; 221:591–598.
8. Aul RB, Oko R. The major subacrosomal occupant of bull spermatozoa is a novel histone H2B variant associated with the forming acrosome during spermiogenesis. Dev Biol 2002; 242:376–387.
9. Mountjoy JR, Xu W, McLeod D, Hyndman D, Oko R. RAB2A: a major subacrosomal protein of bovine spermatozoa implicated in acrosomal biogenesis. Biol Reprod 2008; 79:223–232.
10. Oko R, Maravei D. Protein composition of the perinuclear theca of bull spermatozoa. Biol Reprod 1994; 50:1000–1014.
11. Oko R, Maravei D. Distribution and possible role of perinuclear theca proteins during bovine spermiogenesis. Microsc Res Tech 1995; 32: 520–532.
12. Oko R. Developmental expression and possible role of perinuclear theca proteins in mammalian spermatozoa. Reprod Fertil Dev 1995; 7:777–797.
13. Oko R. Occurrence and formation of cytoskeletal proteins in mammalian spermatozoa. Andrologia 1998; 30:193–206.
14. Oko R, Sutovsky P. Biogenesis of sperm perinuclear theca and its role in sperm functional competence and fertilization. J Reprod Immunol 2009; 83:2–7.
15. Oko R, Donald A, Xu W, van der Spoel AC. Fusion failure of dense-core proacrosomal vesicles in an inducible mouse model of male infertility. Cell Tissue Res 2011; 346:119–134.
16. Robbins J, Dilworth SM, Laskey RA, Dingwall C. Two interdependent basic domains in nucleoplasmin nuclear targeting sequence: identification of a class of bipartite nuclear targeting sequence. Cell 1991; 64:615–623.
17. Dingwall C, Laskey RA. Nuclear targeting sequences—a consensus? Trends Biochem Sci 1991; 16:478–481.
18. Dilworth SM, Dingwall C. Chromatin assembly in vitro and in vivo. Bioessays 1988; 9:44–49.
19. Goldfarb DS, Corbett AH, Mason DA, Harreman MT, Adam SA. Importin alpha: a multipurpose nuclear-transport receptor. Trends Cell Biol 2004; 14:505–514.
20. Gorlich D, Kutay U. Transport between the cell nucleus and the cytoplasm. Annu Rev Cell Dev Biol 1999; 15:607–660.
21. Gorlich D, Prehn S, Laskey RA, Hartmann E. Isolation of a protein that is essential for the first step of nuclear protein import. Cell 1994; 79: 767–778.
22. Weis K, Mattaj IW, Lamond AI. Identification of hSRP1 alpha as a functional receptor for nuclear localization sequences. Science 1995; 268: 1049–1053.
23. Jans DA, Xiao CY, Lam MH. Nuclear targeting signal recognition: a key control point in nuclear transport? Bioessays 2000; 22:532–544.
24. Major AT, Whiley PA, Loveland KL. Expression of nucleocytoplasmic transport machinery: clues to regulation of spermatogenic development. Biochim Biophys Acta 2011; 1813:1668–1688.
25. Hogarth CA, Calanni S, Jans DA, Loveland KL. Importin alpha mRNAs have distinct expression profiles during spermatogenesis. Dev Dyn 2006; 235:253–262.
26. Conti E, Muller CW, Stewart M. Karyopherin flexibility in nucleocytoplasmic transport. Curr Opin Struct Biol 2006; 16:237–244.
27. Conti E, Uy M, Leighton L, Blobel G, Kuriyan J. Crystallographic analysis of the recognition of a nuclear localization signal by the nuclear import factor karyopherin alpha. Cell 1998; 94:193–204.
28. Herold A, Truant R, Wiegand H, Cullen BR. Determination of the functional domain organization of the importin alpha nuclear import factor. J Cell Biol 1998; 143:309–318.
29. Harreman MT, Cohen PE, Hodel MR, Truscott GJ, Corbett AH, Hodel AE. Characterization of the auto-inhibitory sequence within the N-terminal domain of importin alpha. J Biol Chem 2003; 278:21361–21369.
30. Cingolani G, Petosa C, Weis K, Muller CW. Structure of importin-beta bound to the IBB domain of importin-alpha. Nature 1999; 399:221–229.
31. Gorlich D, Henklein P, Laskey RA, Hartmann EA. 41 amino acid motif in importin-alpha confers binding to importin-beta and hence transit into the nucleus. EMBO J 1996; 15:1810–1817.
32. Chook YM, Blobel G. Karyopherins and nuclear import. Curr Opin Struct Biol 2001; 11:703–715.
33. Tomic M, Sunjevaric I, Savtchenko ES, Blumenberg M. A rapid and simple method for introducing specific mutations into any position of DNA leaving all other positions unaltered. Nucleic Acids Res 1990; 18: 1656.
34. Stemmer WP, Morris SK. Enzymatic inverse PCR: a restriction site independent, single-fragment method for high-efficiency, site-directed mutagenesis. Biotechniques 1992; 13:214–220.
35. Hughes MJ, Andrews DW. Creation of deletion, insertion and substitution mutations using a single pair of primers and Biotechniques PCR. 1996; 20: 188, 192–196.
36. Romrell LJ, Bellve AR, Fawcett DW. Separation of mouse spermatogenic cells by sedimentation velocity. A morphological characterization. Dev Biol 1976; 49:119–131.
37. Tovich PR, Oko RJ. Somatic histones are components of the perinuclear theca in bovine spermatozoa. J Biol Chem 2003; 278:32431–32438.
38. Laemmli UK. Cleavage of structural proteins during the assembly of the head of bacteriophage T4. Nature 1970; 227:680–685.
39. Towbin H, Staehelin T, Gordon J. Electrophoretic transfer of proteins from polyacrylamide gels to nitrocellulose sheets: procedure and some applications. Proc Natl Acad Sci U S A 1979; 76:4350–4354.
40. Tovich PR, Sutovsky P, Oko RJ. Novel aspect of perinuclear theca assembly revealed by immunolocalization of non-nuclear somatic histones during bovine spermiogenesis. Biol Reprod 2004; 71:1182–1194.
41. Yang WX, Sperry AO. C-terminal kinesin motor KIFC1 participates in acrosome biogenesis and vesicle transport. Biol Reprod 2003; 69: 1719–1729.
42. Yu Y, Xu W, Yi YJ, Sutovsky P, Oko R. The extracellular protein coat of the inner acrosomal membrane is involved in zona pellucida binding and penetration during fertilization: characterization of its most prominent polypeptide (IAM38). Dev Biol 2006; 290:32–43.

43. Ramalho-Santos J, Schatten G, Moreno RD. Control of membrane fusion during spermiogenesis and the acrosome reaction. Biol Reprod 2002; 67: 1043–1051.
44. Moreno RD, Ramalho-Santos J, Sutovsky P, Chan EK, Schatten G. Vesicular traffic and golgi apparatus dynamics during mammalian spermatogenesis: implications for acrosome architecture. Biol Reprod 2000; 63:89–98.
45. Fontes MR, Teh T, Kobe B. Structural basis of recognition of monopartite and bipartite nuclear localization sequences by mammalian importin-alpha. J Mol Biol 2000; 297:1183–1194.
46. Dingwall C, Laskey RA. Nuclear targeting sequences—a consensus? Trends Biochem Sci 1991; 16:478–481.
47. Koike M, Ikuta T, Miyasaka T, Shiomi T. The nuclear localization signal of the human Ku70 is a variant bipartite type recognized by the two components of nuclear pore-targeting complex. Exp Cell Res 1999; 250: 401–413.
48. Robbins J, Dilworth SM, Laskey RA, Dingwall C. Two interdependent basic domains in nucleoplasmin nuclear targeting sequence: identification of a class of bipartite nuclear targeting sequence. Cell 1991; 64:615–623.
49. Moroianu J, Hijikata M, Blobel G, Radu A. Mammalian karyopherin alpha 1 beta and alpha 2 beta heterodimers: alpha 1 or alpha 2 subunit binds nuclear localization signal and beta subunit interacts with peptide repeat-containing nucleoporins. Proc Natl Acad Sci U S A 1995; 92:6532–6536.
50. Riddick G, Macara IG. The adapter importin-alpha provides flexible control of nuclear import at the expense of efficiency. Mol Syst Biol 2007; 3:118.
51. Lange A, Mills RE, Lange CJ, Stewart M, Devine SE, Corbett AH. Classical nuclear localization signals: definition, function, and interaction with importin alpha. J Biol Chem 2007; 282:5101–5105.
52. Hubner S, Smith HM, Hu W, Chan CK, Rihs HP, Paschal BM, Raikhel NV, Jans DA. Plant importin alpha binds nuclear localization sequences with high affinity and can mediate nuclear import independent of importin beta. J Biol Chem 1999; 274:22610–22617.
53. Kotera I, Sekimoto T, Miyamoto Y, Saiwaki T, Nagoshi E, Sakagami H, Kondo H, Yoneda Y. Importin alpha transports CaMKIV to the nucleus without utilizing importin beta. EMBO J 2005; 24:942–951.
54. Moreno RD, Palomino J, Schatten G. Assembly of spermatid acrosome depends on microtubule organization during mammalian spermiogenesis. Dev Biol 2006; 293:218–227.
55. Fawcett DW. The mammalian spermatozoon. Dev Biol 1975; 44:394–436.
56. Cavicchia JC, Morales A. Characterization of nuclear pore distribution in freeze-fracture replicas of seminiferous tubules isolated by transillumination. Tissue Cell 1992; 24:75–84.
57. Fawcett DW, Chemes HE. Changes in distribution of nuclear pores during differentiation of the male germ cells. Tissue Cell 1979; 11:147–162.
58. Sutovsky P, Ramalho-Santos J, Moreno RD, Oko R, Hewitson L, Schatten G. On-stage selection of single round spermatids using a vital, mitochondrion-specific fluorescent probe MitoTracker(TM) and high resolution differential interference contrast microscopy. Hum Reprod 1999; 14:2301–2312.
59. Cai Y, Gao Y, Sheng Q, Miao S, Cui X, Wang L, Zong S, Koide SS. Characterization and potential function of a novel testis-specific nucleoporin BS-63. Mol Reprod Dev 2002; 61:126–134.
60. Fan F, Liu CP, Korobova O, Heyting C, Offenberg HH, Trump G, Arnheim N. cDNA cloning and characterization of Npap60: a novel rat nuclear pore-associated protein with an unusual subcellular localization during male germ cell differentiation. Genomics 1997; 40:444–453.
61. Kang-Decker N, Mantchev GT, Juneja SC, McNiven MA, van Deursen JM. Lack of acrosome formation in Hrb-deficient mice. Science 2001; 294:1531–1533.
62. Fritz CC, Zapp ML, Green MR. A human nucleoporin-like protein that specifically interacts with HIV Rev. Nature 1995; 376:530–533.
63. Bednenko J, Cingolani G, Gerace L. Nucleocytoplasmic transport: navigating the channel. Traffic 2003; 4:127–135.
64. Kierszenbaum AL, Rivkin E, Tres LL. Acroplaxome, an F-actin-keratin-containing plate, anchors the acrosome to the nucleus during shaping of the spermatid head. Mol Biol Cell 2003; 14:4628–4640.
65. Kierszenbaum AL, Tres LL, Rivkin E, Kang-Decker N, van Deursen JM. The acroplaxome is the docking site of Golgi-derived myosin Va/Rab27a/b- containing proacrosomal vesicles in wild-type and Hrb mutant mouse spermatids. Biol Reprod 2004; 70:1400–1410.
66. Oko R, Donald A, Xu W, van der Spoel AC. Fusion failure of dense-cored proacrosomal vesicles in an inducible mouse model of male infertility. Cell Tissue Res 2011; 346:119–134.
67. Frohnert C, Schweizer S, Hoyer-Fender S. SPAG4L/SPAG4L-2 are testis-specific SUN domain proteins restricted to the apical nuclear envelope of round spermatids facing the acrosome. Mol Hum Reprod 2011; 17: 207–218.
68. Razafsky D, Hodzic D. Bringing KASH under the SUN: the many faces of nucleo-cytoskeletal connections. J Cell Biol 2009; 186:461–472.
69. Fan S, Whiteman EL, Hurd TW, McIntyre JC, Dishinger JE, Liu CJ, Martens JR, Verhey KJ, Sajjan U, Margolis BL. Induction of Ran GTP drives ciliogenesis. Mol Biol Cell 2011; DOI 10.1091/mbc.E11-03-0267.
70. Hurd TW, Fan S, Margolis BL. Localization of retinitis pigmentosa 2 to cilia is regulated by Importin beta2. J Cell Sci 2011; 124:718–726.
71. Dishinger JF, Kee HL, Jenkins PM, Fan S, Hurd TW, Hammond JW, Truong YN, Margolis B, Martens JR, Verhey KJ. Ciliary entry of the kinesin-2 motor KIF17 is regulated by importin-beta2 and RanGTP. Nat Cell Biol 2010; 12:703–710.
72. Fan S, Fogg V, Wang Q, Chen XW, Liu CJ, Margolis B. A novel Crumbs3 isoform regulates cell division and ciliogenesis via importin beta interactions. J Cell Biol 2007; 178:387–398.
73. Keryer G, Di FB, Celati C, Lechtreck KF, Mogensen M, Delouvee A, Lavia P, Bornens M, Tassin AM. Part of Ran is associated with AKAP450 at the centrosome: involvement in microtubule-organizing activity. Mol Biol Cell 2003; 14:4260–4271.